Articles

Crystal Structure of *trans*-$Fe(CO)_3(PPh_3)_2$, Tricarbonylbis(triphenylphosphine)iron(0), and ab Initio Study of the Bonding in *trans*-$Fe(CO)_3(PH_3)_2$

Rainer Glaser,* Young-Hee Yoo,[1a] Grace Shiahuy Chen,[1a] and Charles L. Barnes[1b]

Department of Chemistry, University of Missouri—Columbia, Columbia, Missouri 65211

Received December 22, 1993®

The selective one-step preparation of *trans*-$Fe(CO)_3(PPh_3)_2$, 1, in the absence of $Fe(CO)_4(PPh_3)$ has made it possible to obtain 1 pure and in crystalline form. *trans*-$Fe(CO)_3(PPh_3)_2$ crystallizes in the orthorhombic space group *Pbca* with cell parameters a = 18.216(5) Å, b = 17.0380(10) Å, c = 21.804(3) Å, and Z = 8; R = 0.042 and R_w = 0.056 for 3891 independent reflections with $I > 2.0\sigma(I)$. The crystal structure of 1 is compared to $Ru(CO)_3(PPh_3)_2$, $Os(CO)_3(PPh_3)_2$, $Fe(CO)_2(CS)(PPh_3)_2$, and a selection of complexes of the types *trans*-$Fe(CO)_3(PR_3)_2$ (R = Ph, NMe_2, OMe) and *trans*-$Fe(CO)_4PR_3$ (R = Ph, NMe_2, CMe_3, $SiMe_3$). Effects of equatorial CO substitution in 1 by the diazonium ion and nitrile ligands are discussed. Ab initio calculations that employ effective core potential basis sets at the Hartree–Fock level and which include perturbational corrections for electron correlation at the MP2 level are reported for *trans*-$Fe(CO)_3(PH_3)_2$. Good agreement between theory and experiment can only be obtained at correlated levels of theory in conjunction with double-ζ quality basis sets on iron and all ligands. Population analyses are employed to examine the effects of electron correlation and to delineate the iron–ligand bonding. Electron correlation serves overall to reduce the molecular quadrupole moment. Comparison between the crystal structure of 1 and the theoretical structure of the model system allow differentiation between intrinsic structural preferences and packing effects. In particular, the comparison points out that the Fe–P bond length differences and the nonlinearity of the P–Fe–P backbone are not intrinsic bonding features but are caused by the packing.

Introduction

Bis(phosphine)metal carbonyl complexes such as $Fe(CO)_3(PPh_3)_2$ are important synthetic substrates, and they play crucial roles for example in studies of alkene hydrosilation. Our interest in $Fe(CO)_3(PPh_3)_2$ concerns the substitution chemistry with diazonium ligands leading to iron–diazo complexes. Studies of the electronic structures of diazonium ions led us to propose a new bonding model[2] that has since been tested using theoretical[3] and experimental[4,5] methods. To further probe the electronic structures of diazonium ions and of related systems,[6] the study of their electronic relaxation upon complexation to transition metals[7] is revealing. Ab initio studies and electronic structure analysis of transition metal complexes still pose considerable challenges. These studies largely rely on effective core potentials, and their performance still requires critical examination. Although the method proved successful in many cases,[8] it remains pertinent that such theoretical studies are accompanied by and judged against experimental results.

We selected to investigate first the electronic consequences of CO substitution in *trans*-$Fe(CO)_3(PPh_3)_2$ by aryldiazonium ions. The structure of the $[Fe(CO)_2(N_2C_6H_5)(PPh_3)_2][BF_4]$ salt[9] was reported by Haymore

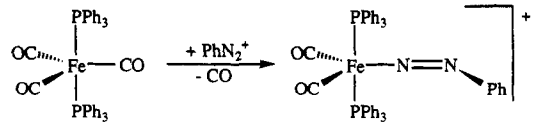

and Ibers.[10] For our purposes it was essential to know the crystal structure of the organometallic precursor and we have now determined its structure. In this article we report the crystal structure of *trans*-$Fe(CO)_3(PPh_3)_2$, 1, and structural comparisons are made to $Os(CO)_3(PPh_3)_2$, $Ru(CO)_3(PPh_3)_2$, and $Fe(CO)_2(CS)(PPh_3)_2$, and within the

• Abstract published in *Advance ACS Abstracts*, May 15, 1994.

(1) (a) Parts of the projected dissertations of Y.H.Y. and G.S.C. (b) Crystallography. (c) Part 1 of the series "Transition Metal Complexes of Diazonium Ions". (d) Presented in part at the 28th Midwest Regional Meeting of the American Chemical Society, November 12, 1993.

(2) (a) Glaser, R. *J. Phys. Chem.* **1989**, *93*, 7993–8003. (b) Glaser, R. *J. Comput. Chem.* **1990**, *11*, 663–679. (c) Glaser, R.; Choy, G. S.-C.; Hall, M. K. *J. Am. Chem. Soc.* **1991**, *113*, 1109–1120. (d) Glaser, R.; Choy, G. S.-C. *J. Am. Chem. Soc.* **1993**, *115*, 2340–2347.

(3) Glaser, R.; Horan, C. J.; Nelson, E.; Hall, M. K. *J. Org. Chem.* **1992**, *57*, 215–228.

(4) (a) Horan, C. J.; Barnes, C. L.; Glaser, R. *Chem. Ber.* **1993**, *126*, 243–249. (b) Horan, C. J.; Barnes, C. L.; Glaser, R. *Acta Crystallogr.* **1993**, *C49*, 507–509. (c) Horan, C. J.; Haney, P. E.; Barnes, C. L.; Glaser, R. *Acta Crystallogr.* **1993**, *C49*, 1525–1528.

(5) (a) Glaser, R.; Chen, G. S.; Barnes, C. L. *Angew. Chem., Int. Ed. Engl.* **1992**, *31*, 740–743. (b) Chen, G. S.; Glaser, R.; Barnes, C. L. *J. Chem. Soc., Chem. Commun.* **1993**, 1530–1532.

(6) Glaser, R.; Horan, C. J.; Haney, P. E. *J. Phys. Chem.* **1993**, *97*, 1835–1844.

(7) Review on organometallic diazo compounds: Sutton, D. *Chem. Rev.* **1993**, *93*, 995–1023.

(8) Veillard, A. *Chem. Rev.* **1991**, *91*, 743–766.

(9) Fisher, D. R.; Sutton, D. *Can. J. Chem.* **1973**, *51*, 1697–1703.

(10) Haymore, B. L.; Ibers, J. A. *Inorg. Chem.* **1975**, *14*, 1369–1376.

0276-7333/94/2313-2578$04.50/0

series of the complexes *trans*-Fe(CO)$_3$E$_2$ [E = PPh$_3$, P(NMe$_2$)$_3$, P(OMe)$_3$] and *trans*-Fe(CO)$_4$E [E = PPh$_3$, P(NMe$_2$)$_3$, P(CMe$_3$)$_3$, P(SiMe$_3$)$_3$]. The structural trends and characteristic features revealed by these comparative analyses will allow us to judge the quality of future ab initio theoretical studies. Our theoretical studies of the ligand exchange reaction will consider *trans*-Fe(CO)$_3$(PH$_3$)$_2$ with the parent phosphine instead of the triphenylphosphine to reduce computational demand. Ab initio results are reported for the *trans*-Fe(CO)$_3$(PH$_3$)$_2$ system by employing effective core potential basis sets at the Hartree–Fock level and with the inclusion of perturbational corrections for electron correlations at the second-order Møller–Plesset (MP2) level. It is found that especially the metal–phosphine distances are extremely dependent on the choice of the theoretical level. Good agreement between theory and experiment can only be obtained at correlated levels of theory and in conjunction with the use of double-ζ quality basis sets. Electron density analyses methods are employed to gain insights into the effects of electron correlation and to examine the bonding.

Experimental and Computational Methods

X-ray Structure Determination of *trans*-Fe(CO)$_3$(PPh$_3$)$_2$ (1). An orange crystal of dimensions 0.35 × 0.35 × 0.35 mm^3 was selected for X-ray diffraction. Data were collected on a Nonius diffractometer with λ(Mo Kα) = 0.709 30 Å. Cell dimensions were obtained from 25 reflections with 20.00° ≤ 2θ ≤ 30.00°. The important parameters of the data collection are collected in Table 1. A total of 4697 reflections were collected, and 3891 unique reflections with $I > 2.0\sigma(I)$ were used. Absorption corrections were made using the θ/2θ scan mode (T_{min} = 0.918 078, T_{max} = 0.997 809; μ = 5.7 cm^{-1}). The residuals for independent reflections with $I > 2.0\sigma(I)$ were R = 0.042, R_w = 0.056. Scattering factors were taken from ref 11. Computer programs were NRCVAX.[12]

Ab Initio Computations. Restricted Hartree–Fock (RHF) calculations were performed with the ab initio quantum-mechanical program Gaussian92[13] on IBM/RS-6000 Models 560 and 580 using direct methods. Electronic structures were analyzed with the Mulliken and natural population[14] basis set partitioning techniques. A nonrelativistic effective core potential (ECP) was used for the basis set of Fe, as described by Hay and Wadt[15] with the valence orbitals 3d, 4s, and 4p. This iron valence basis set is of the type (3s2p5d) and [spd] contracted. The ECP valence basis set of P is of the type (3s3p) and [sp] contracted.[16] These Fe and P basis sets were used in conjunction with the all-electron STO-3G minimal basis sets for C, O, and H, and the resulting basis sets are referred to as the minimal basis set LANL1MB. We also used the same ECPs together with a less contracted valence basis sets for Fe and P that included the same primitives, but the primitives with the lowest exponent were treated as independent basis functions. Thus, Fe and P were assigned [2s2p2d] and [2s2p] valence basis sets, respectively, and these larger basis sets were used in combination with the all-electron double-ζ basis sets[17] on the atoms H, C, and O. The resulting basis sets are commonly denoted LANL1DZ. Sets of six Cartesian d-type functions were used. The (10s,5p)/[3s2p] basis sets of C and O, the (3s3p)/[2s2p] valence basis for P, and the 31G basis for H should provide sufficient flexibility for the description of these atoms, and no additional polarization functions were added in the present work for these atoms. Recent results by Hay[18] suggest that an improvement in the accuracy can be obtained by using the LANL2DZ basis set.[19] At this level, the 3s and 3p orbitals are included in the valence basis set instead of being replaced by effective core potentials. The valence basis set of Fe thus included the 3s, 3p, 3d, and 4s (but not 4p) orbitals and was of the form (8s5p5d)/[3s3p2d]. Phosphorus is described by the same valence basis set of the form (3s3p)/[2s2p] just like at the LANL1DZ level. The basis sets used for H, C, and O at this LANL2DZ level are of the STO-3G type as with the LANL1MB level, that is (6s3p)/[2s1p] for C and O and (3s)/[1s] for H. It will be interesting to examine whether the improvement in the Fe basis is beneficial despite the reduced flexibility in the CO descriptions.

Table 1. Experimental Details

cryst shape and size (mm)	orange, 0.35 × 0.35 × 0.35
chemical formula	$C_{39}H_{30}O_3P_2Fe$
fw	664.45
cryst syst	orthorhombic
space group	*Pbca*
unit-cell dimens (Å)	a = 18.216(5), b = 17.038(1), c = 21.804(3)
no. and θ range (deg) of reflns used for measuring lattice param	25 reflections, 20 ≤ θ ≤ 30
vol of unit cell (Å^3)	6767(2)
Z	8
D_x (g/cm^3)	1.304
radiation and wavelength (Å)	λ(Mo Kα) = 0.709 30
linear abs coeff (cm^{-1})	5.7
temp of measurement (K)	298
method used to measure diffraction data	θ/2θ scans
abs corr type	T_{max} = 0.998, T_{min} = 0.918
no. of reflns measd	4697
no. of ind reflns	4697
no. of obsd reflns	3891
criterion for recognizing obsd reflns	$I > 2.0\sigma(I)$
max value of θ (deg)	$2\theta_{max}$ = 46
range of h, k, and l	0 ≤ h ≤ 20, 0 ≤ k ≤ 18, 0 ≤ l ≤ 23
use of F, F^2 or I	refinement of F
R [=Σ(‖F_o| − |F_c‖)/Σ|F_o|]	0.042
R_w {=[Σ(w|Y_m − Y_c|^2)/Σ(wY^2_m)]$^{1/2}$}	0.056
method of refining and locating H atoms	calcd and included as fixed contribution
no. of reflns used in refinement	3891
S {=[Σw(|Y_m| − |Y_c|)^2/(m − n)]$^{1/2}$}	1.79
max Δ/σ (%)	1.8
max and min Δρ in final diff electron density map (e/Å^3)	max = 0.93 and min = −0.30

Results and Discussion

Crystal Structure of *trans*-Fe(CO)$_3$(PPh$_3$)$_2$. The substitution of Fe(CO)$_5$ by phosphines leading to mixtures of (PPh$_3$)Fe(CO)$_4$ and (PPh$_3$)$_2$Fe(CO)$_3$ has long been known,[20] and there were many attempts to prepare each product in pure form. (PPh$_3$)$_2$Fe(CO)$_3$ is formed primarily when an excess of the phosphine is used,[21] but this and

(11) *International Tables for X-ray Crystallography*; Kynoch Press: Birmingham: U.K., 1974; Vol. IV (present distributor D. Reidel, Dordrecht, The Netherlands).
(12) Gabe, E. J.; Le Page, Y.; Charland, J-P.; Lee, F. L.; White, P. S. *J. Appl. Crystallogr.* **1989**, *22*, 384–387.
(13) *Gaussian92*; Frisch, M. J., Trucks, G. W., Head-Gordon, M., Gill, P. M. W., Wong, M. W., Foresman, J. B., Johnson, B. G., Schlegel, H. B., Robb, M. A., Replogle, E. S., Gomberts, R., Andres, J. L., Raghavachari, K., Binkley, J. S., Gonzalez, C., Martin, R. L., Fox, B. J., Defrees, D. J., Baker, J., Stewart, J. J. P., Pople, J. A., Eds.; Gaussian Inc.: Pittsburgh, PA, 1992.
(14) Review: Weinhold, F.; Carpenter, J. E. In *The Structure of Small Molecules and Ions;* Naaman, R., Vager, Z., Eds.; Plenum Press: New York, 1988, p 227ff.
(15) Hay, P. J.; Wadt, W. R. *J. Chem. Phys.* **1985**, *82*, 270–283.
(16) Wadt, W. R.; Hay, P. J. *J. Chem. Phys.* **1985**, *82*, 284–298.
(17) Dunning, T. H.; Hay, P. J. *Modern Theoretical Chemistry*, Plenum: New York, 1976.
(18) Hay, P. J. *New J. Chem.* **1991**, *15*, 735–740.
(19) Hay, P. J.; Wadt, W. R. *J. Chem. Phys.* **1985**, *82*, 299–310.
(20) Manuel, T. A. *Inorg. Chem.* **1963**, *2*, 854–858.
(21) (a) Clifford, A. F.; Mukherjee, A. K. *Inorg. Chem.* **1963**, *2*, 151–153. (b) Clifford, A. F.; Mukherjee, A. K. *Inorg. Synth.* **1966**, *8*, 185–191.

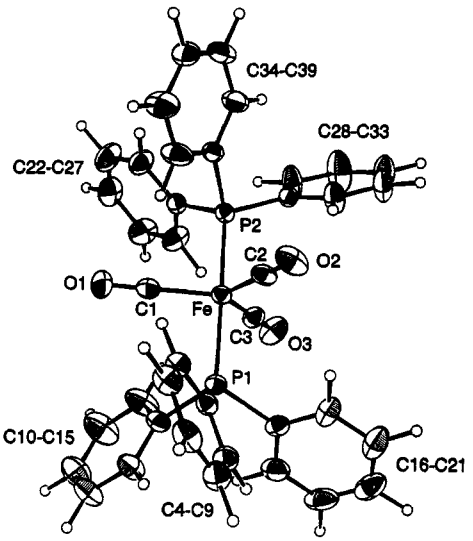

Figure 1. Perspective view of *trans*-$(PPh_3)_2Fe(CO)_3$ with numbering scheme. Thermal ellipsoids are drawn at the 30% probability level.

other methods[22] require vacuum sublimation for purification, while others rely on selective precipitation[23] or chromatography.[24] The selective synthesis of the disubstituted product *trans*-$(PPh_3)_2Fe(CO)_3$ *without* formation of $(PPh_3)Fe(CO)_4$ was recently achieved by Keiter et al. via the one-step reaction of $Fe(CO)_5$ with PPh_3 and $NaBH_4$[25] or NaOH[26] in refluxing *n*-butanol. This method expands on the known improvement in the control of the ratio of mono- versus disubstitution first described by Siegl,[27] which consisted of treating $Fe(CO)_5$ with $LiAlH_4$ or $NaBH_4$ in refluxing THF. The same product also can be obtained by treatment $KHFe(CO)_4$ with the respective phosphine in ethanol.[28] Single crystals of $(PPh_3)_2Fe(CO)_3$ formed very slowly in a $CDCl_3$ solution which was kept in a refrigerator for 2 months.

A perspective ORTEPII[29] drawing of **1** with the numbering scheme and a stereo PLUTO[30] molecular packing diagram are shown in Figures 1 and 2. Final positional parameters are summarized in Table 2, and selected bond lengths, angles, and torsional angles are collected in Table 3.

The local symmetry of the *trans*-$(PPh_3)_2Fe(CO)_3$ trigonal bipyramidal monomers in the unit cell deviates significantly from C_3 symmetry since the P–Fe–P backbone is nonlinear. The P1–Fe–P2 angle is 172.6°, and the distortion is best described as a shift of the P atoms that leaves C1, Fe, and the P atoms coplanar and increases the C2–Fe–P angles. In Figure 3, the orientation was therefore chosen such that C2, Fe, and the P atoms lie in the paper plane. The monomers do not assume approximate C_s symmetry with regard to that plane, as can be seen from the Newman projection depicted in Figure 3. While the two phosphines very nearly are eclipsed with regard to

Table 2. Positional and Equivalent Thermal Parameters with Esd's in Parentheses

atom	*x*	*y*	*z*	*B* or B_{eq}[a] (Å^2)
Fe	0.91245(2)	0.32037(3)	0.14693(2)	2.82(2)
P1	0.93865(4)	0.25747(5)	0.06048(4)	3.01(3)
P2	0.89312(4)	0.39657(5)	0.22761(4)	2.80(3)
C1	0.8287(2)	0.3534(2)	0.1148(2)	4.0(2)
O1	0.7749(2)	0.3734(2)	0.0941(1)	6.9(2)
C2	0.9111(2)	0.2331(2)	0.1915(2)	3.9(2)
O2	0.9096(2)	0.1777(2)	0.2202(1)	6.1(2)
C3	0.9965(2)	0.3707(2)	0.1387(2)	3.8(2)
O3	1.0516(2)	0.4036(2)	0.1339(1)	5.7(2)
C4	0.8938(2)	0.1636(2)	0.0456(2)	3.2(1)
C5	0.8246(2)	0.1486(2)	0.0707(2)	3.8(2)
C6	0.7893(2)	0.0786(2)	0.0581(2)	4.7(2)
C7	0.8212(2)	0.0231(2)	0.0216(2)	4.9(2)
C8	0.8893(2)	0.0361(2)	−0.0035(2)	5.0(2)
C9	0.9258(2)	0.1066(2)	0.0085(2)	4.3(2)
C10	0.9187(2)	0.3141(2)	−0.0092(2)	3.8(2)
C11	0.8986(2)	0.2795(3)	−0.0636(2)	5.2(2)
C12	0.8821(3)	0.3241(3)	−0.1149(2)	6.5(3)
C13	0.8875(3)	0.4040(3)	−0.1115(2)	7.2(3)
C14	0.9065(3)	0.4389(3)	−0.0588(2)	8.1(3)
C15	0.9216(3)	0.3949(2)	−0.0066(2)	6.3(2)
C16	1.0357(2)	0.2288(2)	0.0520(2)	3.8(2)
C17	1.0649(2)	0.1776(2)	0.0950(2)	5.0(2)
C18	1.1373(2)	0.1525(3)	0.0898(3)	6.4(2)
C19	1.1798(3)	0.1798(3)	0.0418(3)	7.1(3)
C20	1.1520(3)	0.2303(4)	0.0002(2)	7.2(3)
C21	1.0794(2)	0.2551(3)	0.0047(2)	5.9(2)
C22	0.8673(2)	0.4979(2)	0.2090(2)	3.2(1)
C23	0.8043(2)	0.5324(2)	0.2315(2)	5.1(2)
C24	0.7875(3)	0.6097(3)	0.2168(2)	6.5(2)
C25	0.8323(3)	0.6524(2)	0.1808(2)	6.1(2)
C26	0.8945(3)	0.6189(3)	0.1575(2)	6.1(2)
C27	0.9114(2)	0.5420(2)	0.1711(2)	5.1(2)
C28	0.9723(2)	0.4083(2)	0.2786(2)	3.2(1)
C29	1.0012(2)	0.4796(2)	0.2953(2)	6.1(2)
C30	1.0616(3)	0.4830(3)	0.3342(3)	8.7(3)
C31	1.0915(2)	0.4164(3)	0.3576(2)	6.7(3)
C32	1.0619(3)	0.3463(3)	0.3424(2)	6.3(2)
C33	1.0033(2)	0.3420(2)	0.3028(2)	5.3(2)
C34	0.8209(2)	0.3681(2)	0.2809(2)	3.3(2)
C35	0.8236(2)	0.3893(3)	0.3424(2)	5.0(2)
C36	0.7645(2)	0.3713(3)	0.3805(2)	5.8(2)
C37	0.7056(2)	0.3329(3)	0.3591(2)	5.5(2)
C38	0.7024(2)	0.3112(3)	0.2989(2)	6.6(3)
C39	0.7606(2)	0.3279(3)	0.2602(2)	5.6(2)

[a] B_{eq} is the mean of the principal axes of the thermal ellipsoid.

Table 3. Bond Lengths (Å), Angles (deg) and Selected Torsion Angles (deg), with Esd's in Parentheses

Fe–P1	2.2201(9)	Fe–C3	1.765(4)
Fe–P2	2.2144(9)	C1–O1	1.132(5)
Fe–C1	1.770(4)	C2–O2	1.134(5)
Fe–C2	1.776(4)	C3–O3	1.154(5)
P1–Fe–P2	172.56(4)	C1–Fe–C2	118.08(17)
P1–Fe–C1	90.13(11)	C1–Fe–C3	123.56(17)
P1–Fe–C2	93.66(11)	C2–Fe–C3	118.34(17)
P1–Fe–C3	87.80(11)	Fe–C1–O1	179.0(3)
P2–Fe–C1	89.51(11)	Fe–C2–O2	179.3(3)
P2–Fe–C2	93.06(11)	Fe–C3–O3	179.4(3)
P2–Fe–C3	86.21(11)		
P1–Fe–C1–O1	61.1(2)	P2–Fe–C1–O1	−126.4(3)
C2–Fe–C1–O1	−33.1(2)	C3–Fe–C1–O1	148.5(4)
P1–Fe–C2–O2	−132.5(3)	P2–Fe–C2–O2	50.6(2)
C1–Fe–C2–O2	−40.4(2)	C3–Fe–C2–O2	138.0(3)
P1–Fe–C3–O3	−142.3(3)	P2–Fe–C3–O3	42.1(2)
C1–Fe–C3–O3	129.0(3)	C2–Fe–C3–O3	−49.3(2)

(22) (a) Strohmeier, W.; Müller, F. J. *Chem. Ber.* **1969**, *102*, 3613–3615. (b) Butts, S. B.; Shriver, D. F. *J. Organomet. Chem.* **1979**, *169*, 191–197. (c) Lewis, J.; Nyholm, R. S.; Sandhu, S. S.; Stiddard, M. H. B. *J. Chem. Soc.* **1964**, 2825–2827. (d) Conder, H. L.; Darensbourg, M. Y. *J. Organomet. Chem.* **1974**, *67*, 93–97.
(23) Therien, M. J.; Trogler, W. C. *Inorg. Synth.* **1989**, *25*, 173–179.
(24) Albers, M. O.; Coville, N. J.; Ashworth, T. V.; Singleton, E. *J. Organomet. Chem.* **1981**, *217*, 385–390.
(25) Keiter, R. L.; Keiter, E. A.; Hecker, K. H.; Boecker, C. A. *Organometallics* **1988**, *7*, 2466–2469.
(26) Keiter, R. L.; Keiter, E. A.; Boecker, C. A.; Miller, D. R. *Synth. React. Inorg. Met.-Org. Chem.* **1991**, *21*, 473–478.
(27) Siegl, W. *J. Organomet. Chem.* **1975**, *92*, 321–328.
(28) (a) Brunet, J. J.; Kindela, F. B.; Neibecker, D. *J. Organomet. Chem.* **1989**, *368*, 209–212. (b) Brunet, J. J.; Taillefer, M. *J. Organomet. Chem.* **1988**, *348*, C5–C8.
(29) Johnson, C. K. ORTEPII. Report ORNL-5138; Oak Ridge National Laboratory: Oak Ridge, TN, 1976.
(30) Motherwell, W. D. S. PLUTO. Program for plotting crystal and molecular structures. University of Cambridge, England, 1976.

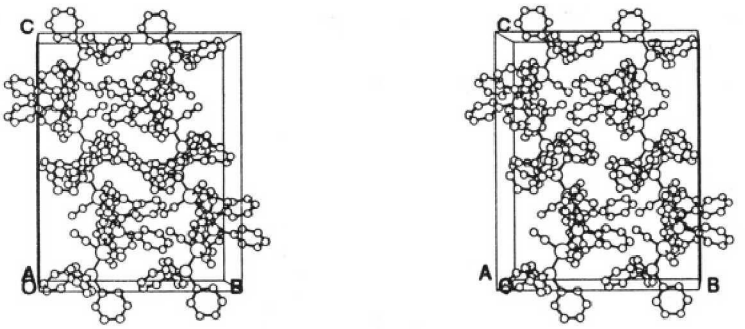

Figure 2. Stereoview of the packing interactions in *trans*-$(PPh_3)_2Fe(CO)_3$.

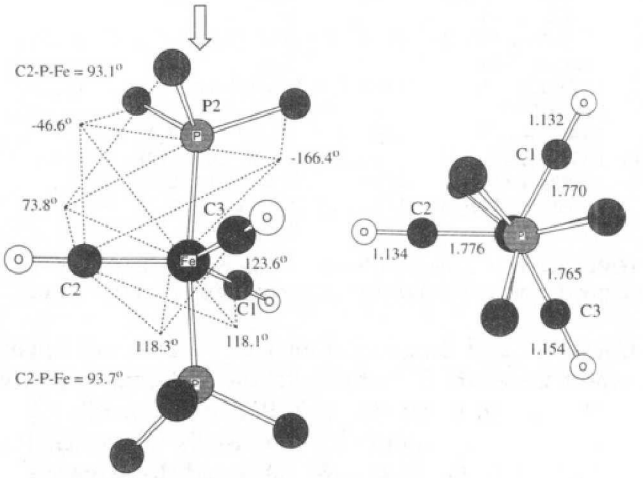

Figure 3. Newman projection of the solid state structure of *trans*-$(PPh_3)_2Fe(CO)_3$ along the direction indicated by the arrow. Phenyl groups omitted for clarity.

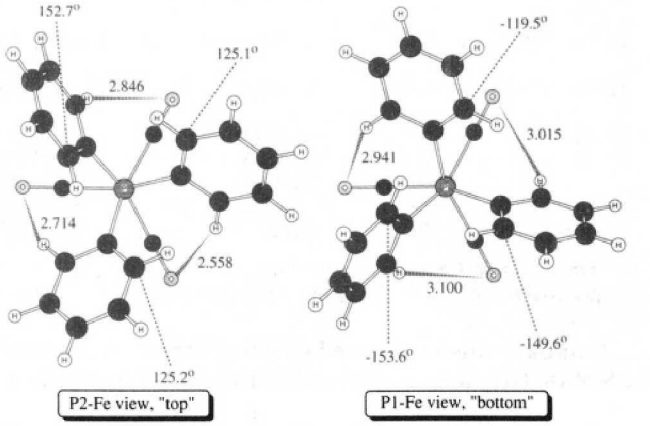

Figure 4. Newman projections of the solid state structure of *trans*-$(PPh_3)_2Fe(CO)_3$ along the P2–Fe and P1–Fe bonds.

each other, it is an interesting feature of this structure that the conformational relation between the nearly trigonal planar and pseudo-D_{3h}-symmetric $Fe(CO)_3$ fragment and the phosphine P–Ph bonds differs very significantly from a staggered arrangement. The dihedral angles between C1, Fe, P2 and the C atoms of the attached phenyl rings are shown in Figure 3. We analyzed the conformations of the axial phosphines in search of an explanation for this characteristic feature. In Figure 4, Newman projections along the P–Fe bonds are shown. The dihedral angles τ, defined as C–P–Fe–C2, are indicated for the three *ortho* carbons that are most remote from the Fe atom, and the distances are given between the hydrogens in the other *ortho* positions and the proximate carbonyl oxygens.[31] The $O–H_{ortho}$ distances vary widely and range from 2.558 to 3.100 Å. The shortest H–O distance of these, involving O3, might be responsible for the elongation of the CO bond length C3–O3 to 1.154 Å compared to the other CO distances of 1.133 ± 0.001 Å (average between the short CO bond lengths of 1.132 and 1.134 Å). The esd's for all of these CO bonds are 0.005 Å (Table 3), and when the worst case scenario is assumed (the long bond is overestimated and the short bonds are underestimated), the difference remains >0.01 Å. Part of this elongation might also be caused by an intermolecular contact between O3 and the *para* hydrogen (H37) of a phenyl group of the molecule at position $(^1/_2 + x, y, ^1/_2 - z)$; the C–O and the H–O distances for this interaction are 3.057 and 2.463 Å, that is, a significantly bent CH---O hydrogen bond. But overall, H-bonding involving the relatively unpolar C–H bonds and the negatively polarized carbonyl oxygens seems of little importance in view of the long distances and, if such intramolecular interactions were important, one would expect a more staggered arrangement about the P–Fe–P backbone. It thus appears that the orientations of the phenyl rings are not consequences of optimizing intramolecular conformation for best steric arrangements but are decided by other factors.

The Newman projection down the P2–Fe bond (Figure 4) nicely shows that two of the phenyl groups have τ values close to 125° while the third is more twisted with τ = 153°. On the other hand, the absolute τ values of the other phosphine indicate just the opposite; two phenyl groups have τ values close to 150° and the remaining Ph group has a small τ value of about 120°. The question as to a potential advantage for these complementary phosphine conformations is not clearly answered by analysis of the packing. There are no strong edge-on arrangements between phenyl groups of neighboring monomers and, in general, the intermolecular contacts show no indication of interactions other than van der Waals interactions.

The nonequivalent phosphine groups in **1** result in slightly different Fe–P bond lengths; they average 2.217 Å with a difference of only 0.006 Å. The Fe–C bond lengths are 1.771 ± 0.005 Å, and the shortest Fe–C bond occurs for that ligand with the longest CO bond length. The crystal structure of **1** allows for instructive comparisons with various similar *trans*-bis(phosphine)iron complexes and with the analogous osmium and ruthenium complexes *trans*-$Os(CO)_3(PPh_3)_2$ and *trans*-$Ru(CO)_3(PPh_3)_2$. Major structural parameters are summarized in Table 4, and esd values are given in this table such that the significance of the comparions can be judged.

(31) For a related discussion of an intramolecular interaction between a piperidine and a coordinated phosphite oxygen, see: Cotton, F. A.; Darensbourg, D. J.; Klein, S.; Kolthammer, B. W. S. *Inorg. Chem.* **1982**, *21*, 1651–1655.

Table 4. Comparison of Major Structural Parameters of Complexes of the Type $(OC)_3MEF$ and Related Systems

no.	M	E	F	M–E	M–F	M–C	C–O	E–M–F	X–P–X	ref
1	Fe	PPh_3	PPh_3	2.2144(9)	2.2201(9)	1.765(4)–1.776(4)	1.132(5)–1.154(5)	172.56(4)	100.33(15)–104.21(16)	this work
2/	Fe[a]	PPh_3	PPh_3	2.232(2)	2.178(2)	1.550(7)–1.766(9)	1.164(9)–1.171(8)	176.08(8)	102.0(3)–104.7(3)	32
				2.185(2)	2.233(2)	1.563(8)–1.778(8)	1.158(8)–1.166(8)	175.02(8)	101.7(3)–105.2(3)	
3/	Os	PPh_3	PPh_3	2.32(4)	2.32(4)	1.90	1.14	180.0	104.4	
				2.42(4)	2.35(4)	1.93(5)	1.27(5)	180.0	102.7–105.2	33
4	Ru	PPh_3	PPh_3	2.330(2)	2.332(2)	1.880(10)–1.925(8)	1.079(10)–1.138(12)	175.73(7)	102.8(2)–103.8(2)	34
5	Ru	PMe_3	PMe_3	2.345(1)	2.334(1)	1.877(6)–1.905(4)	1.142(8)–1.144(5)	178.1(1)	100.5(4)–104.7(7)	35
6	Fe	$P(OCH_3)_3$	$P(OCH_3)_3$	2.155(1)	2.155(1)	1.760(5)	1.153(6)–1.155(9)	179.4(2)	97.6(2)–105.3(2)	36
7	Fe	$P(NMe_2)_3$	$P(NMe_2)_3$	2.213(1)	2.212(1)	1.758(3)–1.761(3)	1.156(4)–1.160(3)	175.1(0)	98.3(1)–110.4(1)	37a
8	Fe	$P(OCH_2)_3P$	$P(OCH_2)_3P$	2.116(4)	2.190(4)	1.78(2)–1.81(1)	1.15(2)	176.4(2)	104.2(4)/100.6(5)	39
9	Fe	$P(NMe_2)_3$	CO	2.245(1)	1.793(6)	1.781(5)–1.792(5)	1.138(6)–1.144(7) axial 1.129(8)	178.1(2)	100.2(2)–105.9(2)	37a
10	Fe	PPh_3	CO	2.244(1)	1.795(4)	1.792(4)–1.796(4)	1.135(5)–1.150(5) axial 1.139(6)	178.3(1)	103.5(1)–104.2(1)	40
11	Fe	$P(CMe_3)_3$	CO	2.364(1)	1.768(4)	1.784(2)–1.805(5)	1.136(6)–1.153(6) axial 1.138(6)	175.7(1)	107.0(2)–107.2(2)	41
12	Fe	$P(SiMe_3)_3$	CO	2.338(4)	1.74(2)	1.77(2)–1.84(2)	1.123(12)–1.15(2) axial 1.15(2)	174.9(6)	105.6(2)–106.6(3)	42
13	Fe	PPh_3	carbene[b]	2.244(1)	1.864(5)	1.744(6)–1.776(6)	1.146(6)–1.169(6)	176.5(2)	101.7(2)–103.7(2)	43a
14/	Fe	PEt_3	carbene[c]	2.202(3)	1.951(10)	1.753(12)–1.800(10)	1.12(2)–1.15(2)	171.5(3)	95.1(8)–104.6(10)	43b
				2.214(3)	1.949(10)	1.757(9)–1.804(12)	1.10(2)–1.15(2)	172.8(3)	96.3(14)–102.2(15)	
15	Fe[d]	PPh_3	PPh_3	2.261(2)	2.266(2)	1.767(9)–1.818(9)	1.138(8)–1.141(8)	175.85(8)	105.3(2)–107.0(2)	10
16	Fe[e]	PEt_3	PEt_3	2.129	2.140	1.709, 1.747	1.137, 1.174	179.3	89.4–105.4	45

[a] One equatorial CS and *trans* phosphines; $Fe(PPh_3)_2(CO)_2CS$. [b] Carbene: $C(OEt)CH(SPh)CH_2Bu$. [c] Carbene: 1,3-dimethyl-2-imidazolidinylidene. [d] Equatorial single-bent PhN_2^+ ligand. [e] Equatorial ethylnitrile. / Two entries are given for cases where the unit cell contains two independent molecules.

Comparisons to Related Crystal Structures. CO/CS Substitution. $Fe(CO)_2(CS)(PPh_3)_2$,[32] **2**, is topologically closely related to **1**. CO/CS replacement strengthens the Fe–CO bonds (av(Fe–C,1) = 1.771 Å, av(Fe–C,2) = 1.665 Å) and lengthens the C–O bonds (av(C–O,1) = 1.143 Å, av(C–O,2) = 1.165 Å). The difference between the Fe–P bonds in **2** is considerably larger (by 0.05 Å) compared to **1**.

Osmium and Ruthenium versus Iron in *trans*-$M(CO)_3(PPh_3)_2$. The complexes $Os(CO)_3(PPh_3)_2$,[33] **3**, $Ru(CO)_3(PPh_3)_2$,[34] **4**, and $Ru(CO)_3(PMe_3)_2$,[35] **5**, are topologically equivalent and isoelectronic with **1**. In going from Fe to Ru all M–L distances increase by about 0.12 Å: The Ru–P bonds (av(Ru–P,4&5) = 2.335 Å) are 0.118 Å longer and the Ru–C bonds (av(Ru–C,4&5) = 1.897 Å) are 0.126 Å longer than those in **1**. In going from Fe to Os all M–L distances increase by about 0.14 Å: The Os–P bonds (av(Os–P,3) = 2.353 Å) are 0.136 Å longer and the Os–C bonds (av(Os–C,3) = 1.915 Å) are 0.144 Å longer than those in **1**. These increases are significantly more than the differences of 0.07 and 0.08 Å in the atomic radii between Fe (1.26 Å) and Ru (1.33 Å) or Os (1.34 Å), respectively. The CO bond lengths do not follow a systematic trend. While one type of molecule **3** shows CO bonds of 1.140 Å, slightly longer than in **1** as expected, the other symmetry-type molecules **3** were reported to exhibit much longer CO bonds of 1.27 Å. **4** shows great differences in the CO bond lengths while the CO distances in **5** all are essentially equal.

Phosphine Ligand Effects in *trans*-$Fe(CO)_3(PX_3)_2$ Complexes. The structural effects of the nature of the phosphines can be examined by comparison of **1** with the complex $Fe(CO)_3(P(OMe)_3)_2$, **6**, reported by Ginderow[36] and the complex $Fe(CO)_3(P(NMe_2)_3)_2$, **7**, reported by Cowley et al.[37] In going from **1** to **7** and **6**, one might expect to see trends that parallel the X electronegativity of PX_3 which might decrease P σ-dative bonding and increase π back-bonding. The average Fe–C bond lengths 1.771 (**1**) > 1.760 (**7**) ≈ 1.760 (**6**) Å and the average CO bond lengths 1.143 (**1**) < 1.156 (**7**) ≈ 1.153 (**6**) Å indicate that the bonding within the $Fe(CO)_3$ units in **6** and **7** is similar but different from **1**.[38] The weaker Fe–CO interactions in **1** are accompanied not by stronger but by longer Fe–P bonds; these bonds become shorter in the order expected on the basis of X electronegativity, 2.217 (**1**) ≈ 2.213 (**7**) > 2.155 (**6**) Å, and this conclusion holds even in light of the standard deviations. This suggests that bonding to Fe is enhanced in **7** because of stronger Fe–CO and in **6** by both stronger Fe–CO bonds and stronger Fe–P bonds (increased back-donation). Verkade's complex[39] **8** is a very exciting system as it allows one to study the consequences of simultaneous Fe–$P(OR)_3$ and Fe–PR_3 complexation. Both the Fe–$P(OR)_3$ and the Fe–PR_3 bonds are shorter than those in **5** and **1**.

***trans*-$Fe(CO)_3(PX_3)_2$ versus $Fe(CO)_4(PX_3)$.** The crystal structures of several tetracarbonyliron complexes with phosphines in axial positions can be used to compare the Fe–P linkages. Complex **7** and $Fe(CO)_4(P(NMe_2)_3)$, **9**,[37a] and complexes **1** and $Fe(CO)_4(PPh_3)$, **10**,[40] are related in the same way, and further comparison can be made to $Fe(CO)_4(P(CMe_3)_3)$, **11**,[41] and $Fe(CO)_4(P(SiMe_3)_3)$, **12**.[42]

(32) Touchard, D.; Fillaut, J.-L.; Dixneuf, P. H.; Toupet, L. *J. Organomet. Chem.* **1986**, *317*, 291–299.
(33) Stalick, J. K.; Ibers, J. A. *Inorg. Chem.* **1969**, *8*, 419–423.
(34) Dahan, F.; Sabo, S.; Chaudret, B. *Acta Crystallogr.* **1984**, *C40*, 786–788.
(35) Jones, R. A.; Wilkinson, G.; Galas, A. M. R.; Hursthouse, M. B.; Malik, K. M. A. *J. Chem. Soc., Dalton Trans.* **1980**, 1771–1778.
(36) Ginderow, P. D. *Acta Crystallogr.* **1974**, *B30*, 2798–2802.
(37) (a) Cowley, A. H.; Davis, R. E.; Remadna, K. *Inorg. Chem.* **1981**, *20*, 2146–2152. (b) Cowley, A. H.; Davis, R. E.; Lattman, M.; McKee, M.; Remadna, K. *J. Am. Chem. Soc.* **1979**, *101*, 5090–5093.
(38) Note that this comparison is based on *average* bond lengths and is not necessarily true for *individual* bonds. For example, the Fe–C bond of 1.765(4) Å in **1** is virtually equal to the Fe–C bond of 1.761(3) Å in **7**. Similarly, the C–O bond of 1.154(5) Å in **1** is virtually equal to the C–O bond of 1.160(3) Å in **7**.
(39) Allison, D. A.; Clardy, J.; Verkade, J. G. *Inorg. Chem.* **1972**, *11*, 2804–2809.
(40) Riley, P. E.; Davis, R. E. *Inorg. Chem.* **1980**, *19*, 159–165.
(41) Pickardt, J.; Rösch, L.; Schumann, H. *J. Organomet. Chem.* **1976**, *107*, 241–248.
(42) Barron, A. R.; Cowley, A. H.; Nunn, C. M. *Acta Crystallogr.* **1988**, *C44*, 750–751.

Table 4 also contains data for two carbene complexes[43] **13** and **14** which are given without comment.

The substitutions of the axial phosphines by CO in **1** and **7** have similar structural consequences in **10** and **9**, respectively, in that the remaining Fe–P bonds lengthen by about 0.03 Å to 2.245 ± 0.001 Å and the apical Fe–C bonds are 1.794 ± 0.001 Å in both tetracarbonyl complexes. The equatorial Fe–C bonds in the $Fe(CO)_4PX_3$ complexes **9** and **10** also are longer by about 0.025 Å compared to those in **7** and **1**, respectively. In $Fe(CO)_4(PPh_3)$, **10**, all Fe–C bonds are essentially of the same length and all CO bonds are within 0.01 Å. For $Fe(CO)_4(P(NMe_2)_3)$, **9**, the average equatorial Fe–C bonds are slightly shorter and the corresponding average CO bonds are longer compared to the apical Fe–CO fragment, but standard deviations are such that these differences are of little significance. The Fe–P bonds become even weaker in **11** and **12** and the *trans*-apical Fe–C bonds become shorter compared to **9** and **10**. Complexes **11** and **12** both demonstrate the strengthening of the *trans*-apical Fe–C bond compared to the equatorial Fe–C bond that is associated with the weakening of the Fe–P bonds; in these cases the *trans*-apical Fe–C are significantly shorter than the equatorial bonds (Table 4).

Effects of CO Substitution by Diazonium and Nitrile Ligands. Our main interest lies with the analysis of the major structural consequences of CO substitution in **1** to obtain the ion **15**. The most significant change is the increase in the Fe–P bond lengths: They lengthen by 0.047 Å from an average of 2.217 Å in **1** to 2.264 Å (2.261 Å and 2.266 Å in **15**). The consequences in the $Fe(CO)_2$ fragment are more modest. The Fe–C bonds lengthen from an average of 1.770 Å in **1** to 1.793 Å (1.818 Å and 1.767 Å in **15**), by 0.023 Å, and the CO bond lengths remain about the same. Very characteristic is an angular change in the $Fe(CO)_2$ fragment: While the C–Fe–C angles in **1** are in the range from 118 to 123°, the C–Fe–C angle in **15** is drastically reduced to 107.6° and the N–Fe–C angles differ by almost 10°. The forthcoming study of the CO/PhN_2^+ substitution reaction will have to reflect these features and explain their origins.[44]

Birk et al. recently reported the crystal structure[45] of $Fe(CO)_2(PEt_3)_2NC$–Et, **16**, which is similar to **15** but contains a neutral nitrile ligand in the equatorial position instead of the diazonium ion (and also PEt_3 instead of PPh_3). The nitrile ligand is probably more of a donor but surely is less back-accepting compared to the diazonium ion because it is neutral and because the polarization mechanism discussed for RNN^+ is not possible. The N–Fe bond in **16** is weaker (1.951 Å) than that in **15**, the Fe–P bonds differ less from those of **1**, and the remaining Fe–C bonds are stronger than those in **1**. In **16**, the C–Fe–C angle is 124.4° and the N–Fe–C angles are 118.2 and 117.4°. The comparison between the different effects of substitution of **1** to give **15** and **16** suggests that the C–Fe–C angle is a crucial parameter for the analysis of the importance of Fe→N back-bonding in **15**.

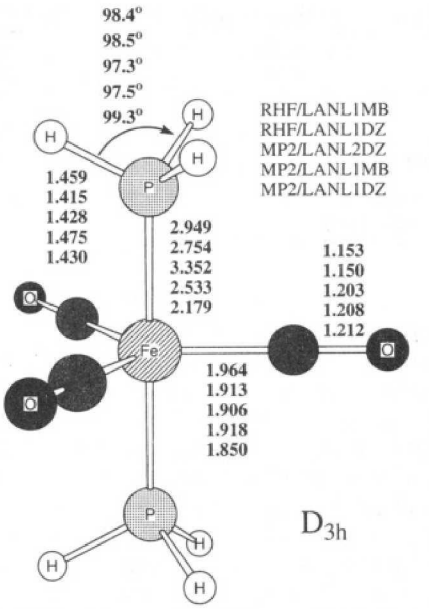

Figure 5. Molecular model of the optimized structure of *trans*-$(OC)_3Fe(PH_3)_2$ with selected structural parameters.

Ab Initio Structure of *trans*-$Fe(CO)_3(PH_3)_2$. For the present ab initio calculations of the structure of **1** and for the forthcoming theoretical investigation of the CO substitution reaction of $Fe(CO)_3(PPh_3)_2$ by the phenyldiazonium ion, the triphenylphosphine ligands render the task too computer-time demanding. We thus replaced PPh_3 by PH_3. Quantitative analyses of the Fe–P bond strengths with dependence on the nature of the phosphines suggest that the replacement of PPh_3 by trialkylphosphines increases the Fe–P bond strength and that this effect reflects primarily electronic rather than steric effects.[46] The effects of the phosphine substitution pattern on a metal–phosphorus bond were examined systematically for the systems *cis*-$Mo(CO)_4(PPh_{3-n}R_n)_2$ where R = Me for n = 0–3, and a modest shortening of the Mo–P bond with increasing n was found.[47] Similar results also were found for the series *cis*-$Mo(CO)_4(PR_3)_2$ with R = Me, Et, *n*-Bu.[48] Theoretical evidence in support of the validity of the PPh_3/PH_3 replacement also is provided by the recent studies of Lin and Hall.[49]

Calculation of $(OC)_3Fe(PH_3)_2$ in D_{3h} symmetry and a staggered arrangement of the phosphines relative to the $Fe(CO)_3$ unit at the RHF/LANL1MB level led to a structure (Figure 5) with *extremely* long Fe–P bond lengths of 2.949 Å. The computation of the Hessian matrix revealed that this structure is not a minimum but exhibits four imaginary frequencies. The first two of these are degenerate (i238 cm^{-1}), and their displacement vectors indicate a P–Fe–P backbone distortion from linearity. The other imaginary modes are nearly degenerate ($\approx i$32 cm^{-1}) and correspond to motions of the phosphines that reduce the symmetry from staggered (relative to the $Fe(CO)_3$ unit) D_{3h} to *gauche* D_{3h} and to C_{3v}, respectively. Use of the

(43) (a) Lotz, S.; Dillen, J. L. M.; van Dyk, M. M. *J. Organomet. Chem.* **1989**, *371*, 371–382. (b) Hitchcock, P. B.; Lappert, M. F.; Thomas, S. A.; Thorne, A. J.; Carty, A. J.; Taylor, N. J. *J. Organomet. Chem.* **1986**, *315*, 27–44.

(44) (a) "Transition Metal Complexes of Diazonium Ions. A Study of the Equatorial CO/PhN_2^+ Exchange Reaction in *Trans*-$Fe(CO)_3(PPh_3)_2$ Using *Ab Initio* Theory and X-Ray Crystallography." Chen, G. S.; Yoo, Y.-H.; Glaser, R. Presentation in the Inorganic Chemistry Division at the Regional Meeting of the American Chemical Society, Columbia, MO, November 1993. (b) Chen, G. S.; Glaser, R. publication in preparation.

(45) Birk, R.; Berke, H.; Hund, H.-U.; Huttner, G.; Zsolnai, L.; Dahlenburg, L.; Behrens, U.; Sielisch, T. *J. Organomet. Chem.* **1989**, *372*, 397–410.

(46) (a) Luo, L.; Nolan, S. P. *Inorg. Chem.* **1993**, *32*, 2410–2415. (b) Luo, L.; Nolan, S. P. *Organometallics* **1992**, *11*, 3483–3486.

(47) Cotton, F. A.; Darensbourg, D. J.; Klein, S.; Kolthammer, B. W. S. *Inorg. Chem.* **1982**, *21*, 294–299.

(48) Cotton, F. A.; Darensbourg, D. J.; Klein, S.; Kolthammer, B. W. S. *Inorg. Chem.* **1982**, *21*, 2661–2666.

(49) (a) Lin, Z.; Hall, M. B. *J. Am. Chem. Soc.* **1992**, *114*, 2928–2932. (b) Lin, Z.; Hall, M. B. *J. Am. Chem. Soc.* **1992**, *114*, 6102–6108.

Table 5. Ab Initio Energies for $(OC)_3Fe(PH_3)_2$[a]

symmetry	theoretical level	energy/ LANL1MB	energy/ LANL1DZ
D_{3h}	RHF	−370.980 162[b]	−375.452 437
D_{3h}	MP2 (full)	−371.681 078[c]	−376.623 253[c]
C_1 (de facto D_{3h})	MP2 (full)		−376.623 252

[a] Total energies in atomic units. [b] Vibrational frequency analysis: VZPE = 50.01 kcal/mol; four imaginary frequencies. [c] E(RHF/LANL1MB) = −370.942970; E(RHF/LANL1DZ) = −375.381631 au.

larger basis set LANL1DZ reduced the Fe–P bond (2.754 Å) somewhat, but the bonds remained much too long. The replacement of PPh_3 by PH_3 certainly cannot be responsible for this elongation but the very long Fe–P bonds suggested that severe systematic problems are indicated at the RHF level. We optimized the staggered D_{3h} structure of $(OC)_3Fe(PH_3)_2$ also with the inclusion of electron correlation effects using the basis sets LANL1MB and LANL1DZ. At the MP2/LANL1MB level, a structure resulted with stronger Fe–P bonds (2.533 Å) but they still remain too long. Good agreement could only be obtained when the electron correlated method was used in conjunction with the larger basis set. At the MP2/LANL1DZ level, the Fe–P bonds are 2.179 Å and in very good agreement (0.04 Å; deviation 1.6%) with the average value of 2.215 Å for the respective bonds in **1**. The PPh_3/PH_3 replacement is anticipated to strengthen the Fe–P bond somewhat (vide supra). At this point the question remained as to whether the staggered D_{3h} structure is indeed a minimum or whether a structure of lower energy exists on the potential energy surface with lower symmetry due to a nonlinear P–Fe–P backbone, different Fe–P bond lengths, or a different conformation. To answer this question, we reoptimized **1** without symmetry constraints (C_1) and started from a significantly distorted structure. After extremely slow convergence—reflecting the very low force constants controlling the conformation of the phosphines—the staggered D_{3h} geometry resulted again. Thus, the staggered D_{3h} structure of $(OC)_3Fe(PH_3)_2$ is a minimum and the preferred structure in the gas phase.

The Fe–C bonds in staggered D_{3h} $(OC)_3Fe(PH_3)_2$ are 1.850 Å, which is somewhat higher (by 4.5%) than the average for **1** (1.770 Å). The C–O bonds are 1.212 Å and longer by about 0.07 Å (or 5.3%) compared to the value of 1.140 Å for **1**. We conclude that the MP2/LANL1DZ level is suitable to predict structures that are in very close agreement with experimental data while the RHF computations completely fail to reproduce even approximate structures.

We also studied staggered D_{3h} $(OC)_3Fe(PH_3)_2$ at the MP2/LANL2DZ level of theory. One might expect that the use of the reduced effective core potential, ECP-2, for Fe and the inclusion of the 3s and 3p Fe orbitals into the valence shell together with the same P basis set as in the LANL1DZ basis set would lead to an even better agreement between theory and experimental data. However, optimizations of D_{3h} $(OC)_3Fe(PH_3)_2$ starting with the Fe–P bond length of 2.179 Å (equilibrium at MP2/LANL1DZ) and incrementing by 0.05 Å for Fe–P distances between 2.079 and 3.279 Å led to a steady energy decrease without even an indication of a shoulder. We attribute the failure of the MP2/LANL2DZ level to the small basis set (STO-3G) used for the description of the CO ligands while the LANL1DZ basis sets for C and O are of (10s,5p)/[3s2p] quality. This finding points out that an accurate reproduction of the structure of $(OC)_3Fe(PH_3)_2$ requires an MP2 treatment in conjunction with good basis sets on the metal *and all the ligands*.

The level dependency of the structure of $(OC)_3Fe(PH_3)_2$ is similar to the case of $Fe(CO)_5$ which was discussed in detail by Lüthi, Siegbahn, and Almlöf,[50] by Ziegler, Tschinke, and Ursenbach,[51] and by Barnes, Rosi, and Bauschlicher.[52] For $Fe(CO)_5$ it is well-known that Hartree–Fock calculations produce Fe–C bonds that are too long. In particular, the axial Fe–C bonds are greatly overestimated in $Fe(CO)_5$ although the tendency toward axial Fe–C "dissociation" is *much less pronounced* than that in $(OC)_3Fe(PH_3)$. Lüthi et al. as well as Barnes et al. found that CI and MCPF treatments result in great improvements of the structure, although questions remain as to the difference between the axial and equatorial bond lengths. The perturbation treatment employed here for the diphosphine system improves the situation in qualitatively the same fashion and results in structures that agree with experimental data equally well. It thus appears that the level MP2/LANL1DZ provides a suitable choice of theoretical level that combines computational efficiency and demand for accuracy in an excellent fashion.

Our theoretical work leads us to conclude that there is an intrinsic preference for a linear P–Fe–P backbone with identical Fe–P bonds in $(OC)_3Fe(PH_3)_2$. This finding suggests that the differences in the Fe–P bond lengths and the slightly bent P–Fe–P backbone found in the solid state structure of **1** reflect packing effects. We emphasize that the relative orientations of the phosphines with respect to the $Fe(CO)_3$ unit are associated with very small force constants and all necessary care must be taken when implications on bonding are deducted on the basis of conformation.

Electronic Structure of *trans*-$Fe(CO)_3(PH_3)_2$. The metal–ligand interactions are usually described in terms of σ-donation from the ligand to the metal center and concomitant π back-bonding, the Dewar–Chatt–Duncanson model. Davidson et al. recently reviewed the transition metal–carbonyl bond, and many pertinent references to metal–carbonyl bonding can be found there.[53] Within this model, the relative weakness of the axial bonds compared to the equatorial bonds is explained by a stronger σ-dative axial bond and increased equatorial π back-bonding.[50] Lüthi et al. employed electron density difference plots for $Fe(CO)_5$ to demonstrate that electron correlation serves to increase the σ-donation from the axial ligands and also to increase in a synergistic fashion the π back-donation in the equatorial bonds. Their theoretical conclusions for $Fe(CO)_5$ are fully supported by our experimental and theoretical study of *trans*-$Fe(CO)_3(PH_3)_2$. Replacement of the axial CO by the mostly σ-dative bonding phosphines should result in much more significant correlation effects on the structure if the explanation for the relative weakness of the axial bonds were correct. Indeed, our results demonstrate that the overestimation of the axial Fe–P bonds at the RHF level is much more significant than that for the axial Fe–C bonds (vide supra). The following electronic structure analysis corroborates the argument

(50) Lüthi, H. P.; Siegbahn, P. E. M.; Almlöf, J. *J. Phys. Chem.* **1985**, *89*, 2156–2161.
(51) Ziegler, T.; Tschinke, V.; Ursenbach, C. *J. Am. Chem. Soc.* **1987**, *109*, 4825–4837.
(52) Barnes, L. A.; Rosi, M.; Bauschlicher, C. W. *J. Chem. Phys.* **1991**, *94*, 2031–2039.
(53) Davidson, E. R.; Kunze, K. L.; Machado, F. B. C., Chakravorty, S. J. *Acc. Chem. Res.* **1993**, *26*, 628–635.

Table 6. Electron Density Analysis

	Mulliken charges			natural charges		
atom or fragment	RHF	MP2	Δ^b	RHF	MP2	Δ^b
		$Fe(CO)_3(PH_3)_2$[a]				
Fe	−0.348	−0.615	0.267	−0.520	−0.760	0.240
P	0.206	0.373	−0.167	0.307	0.498	−0.191
H	0.013	0.011	0.002	0.007	0.002	0.005
PH_3	0.246	0.406	−0.160	0.328	0.504	−0.176
C	0.295	0.078	0.217	0.591	0.333	0.258
O	−0.343	−0.143	−0.200	−0.636	−0.415	−0.221
CO	−0.048	−0.065	0.017	−0.045	−0.082	0.037
		PH_3				
P	0.122	0.098	0.024	0.107	0.099	0.008
H	−0.041	−0.033	−0.008	−0.036	−0.033	−0.003
		CO				
C	0.277	0.065	0.212	0.638	0.416	0.222

[a] Based on the MP2/LANL1DZ structure of *trans*-$Fe(CO)_3(PH_3)_2$. [b] Δ = RHF − MP2.

and, moreover, provides an explanation as to why the stronger axial σ-dative bond does occur at the correlated level.

We performed Mulliken and natural population analyses for the staggered D_{3h} symmetric MP2/LANL1DZ optimized structure of *trans*-$Fe(CO)_3(PH_3)_2$ and also for CO and PH_3. Atom and fragment charges are reported in Table 6 for the MP2/LANL1DZ level as well as for the RHF/LANL1DZ density computed with the MP2/LANL1DZ structures. The comparison between the two data sets obtained with the RHF and MP2 densities allows one to examine the effects of electron correlation on the electronic structure.

Both population analyses provide qualitatively the same description of the intramolecular charge transfer. We discuss the NPA data obtained at the MP2/LANL1DZ level in the following, as they are known to better reflect polarities. The phosphine ligands are severely electron deficient in the complex with an overall PH_3 charge of +0.504, and most of the charge resides on P itself. The equatorial carbonyl ligands carry small negative charges, −0.082, and most of the negative charge is assigned to iron, −0.760. While the phosphine ligand's binding to iron is dominated by σ-dative bonding, the carbonyls σ-dative bonding is overcompensated for by efficient π back-bonding.

The ΔC values in Table 6 give the charge differences at the RHF and MP2 levels, and they indicate where electron density was accumulated ($\Delta C > 0$) or depleted ($\Delta C < 0$) as a result of electron correlation. While the charges vary in absolute magnitude between the two population analyses, the two sets of ΔC obtained are very similar and, as before, we discuss the NPA derived data. The main consequence of electron correlation is an increase of electron density at Fe (ΔC = +0.240) and a decrease of electron density of the PH_3 ligand (ΔC = −0.176). It is this feature, of course, that is responsible for the stronger σ-dative bond at the correlated level, but why does it occur? The effects of electron correlation on the overall charge of the CO ligands are comparatively small electron density increases (ΔC = +0.037) *but a very significant change in the CO bond polarity*: The ΔC(C) = +0.258 and ΔC(O) = −0.221 values show a substantial transfer of electron density from oxygen to carbon! The (+) charge reduction at C is larger than the (−) charge reduction at O; that is, not only does electron correlation reduce the bond polarity C(+)–O(−) but it also makes the C atoms better acceptors. Axial P→Fe σ-dative bonding is reinforced because electron density accumulation on Fe and Fe–C bonding is facilitated and because the electrostatic repulsion between the phosphine ligands and the C(+)–O(−) dipoles is dramatically reduced.

The fundamental properties that govern bonding are *molecular* properties, and nature favors systems with the lowest energy and the most spherical electron density possible. The effects of the electron correlation on the electron density are manifested in the quadrupole moment, Q, a *molecular* property reflecting deviations of the electron density from spherical symmetry. Because of symmetry, the quadrupole moment tensor is reduced to the diagonal elements and two of these are degenerate; Q_{xx} and Q_{zz}, which suffice to describe Q. Q_{xx} reflects primarily the quadrupole associated with the $[O(-)–C(+)]_2Fe(-)–C(+)–O(-)$ unit and Q_{zz} reflects mostly the quadrupolar nature of the P(+)–Fe(−)–P(+) backbone. With the MP2 and RHF densities, these values are Q_{xx} = −84.74 D·Å, Q_{zz} = −55.27 D·Å and Q_{xx} = −88.39 D·Å, Q_{zz} = −56.20 D·Å, respectively. Thus, electron correlation overall reduces the quadrupole moment *of the molecule*; that is, all the changes of the *bond* polarities serve to reduce the *molecular* polarity.

The conclusions drawn from the electronic structure analysis are fully consistent with the structural changes of the ligands as a result of complexation. The PH bond in the complex is 1.430 Å and just slightly shorter compared to that in free PH_3 (1.439 Å) and the angle ∠(H–P–H) = 99.5° is 4.0° larger in the complex. The structures of free and complexed phosphine suggest a tendency to increase the s character of P orbitals used for the PH bonds, which is beneficial for Fe–P bonding. The CO bond length in the complex is 1.212 Å, while it is only 1.189 Å in free CO at the same level. The shortening by 0.023 Å can be understood on the basis of the reduced bond polarity of the coordinated CO. If we take the difference between the atom charges, DAC(XY) = |AC(X) − AC(Y)|, as a simple index for bond polarity, we find a difference of the DAC values between free and coordinated CO of ΔDAC = +0.084. In fact, the situation is very similar *but opposite* to the shortening of the NN bond in diazonium ions compared to free N_2 which we have analyzed previously in detail both experimentally and theoretically.[2-5] In both cases, the coordination involves little overall charge transfer but has major consequences on the *internal* electron density distributions within CO and N_2. While N_2 becomes strongly polarized in the diazonium ions, the polarity of the CO is strongly reduced in the complex. In terms of the bond polarity index, ΔDAC(CO) = +0.084 is *positive* while ΔDAC(NN) = −0.174 is *negative*.[54]

Conclusion

The crystal structure of *trans*-$Fe(CO)_3(PPh_3)_2$ has been determined and analyzed in comparison to its Os and Ru analogs and other related Fe complexes. The comparative analyses revealed important structural trends and features that provide pertinent references to judge the quality of ab initio theoretical studies of these types of systems in general and for our forthcoming work on the CO/RN_2^+ substitution reaction of 1 in particular. Hartree–Fock calculations fail completely to approximate the structure of $Fe(CO)_3(PH_3)_2$ in that the staggered D_{3h} structure is

(54) Values for N_2 and the methyldiazonium ion from the NPA analysis reported in ref 2d at the (comparable) MP2/6-31G* level.

predicted to be a higher order saddle point with extremely long Fe–P bonds. Very good agreement between theory and experiment can be obtained with second-order perturbation theory in conjunction with larger effective core potential basis sets, that is, at the MP2/LANL1DZ level. The failure of the MP2/LANL2DZ level computations is attributed to the small basis sets used for the CO ligands. Population analyses show that electron correlation serves to reinforce P→Fe σ-dative bonding by means of drastically reducing the polarity of the CO bonds and of increasing the acceptor ability of the carbonyl carbons for Fe→C π back-bonding. All of these electron correlation effects serve to reduce the molecular quadrupole moment. The theoretical study suggests that the nonequality of the Fe–P bonds, the modest deviation of the P–Fe–P backbone from linearity, and the deviations from the ideal all-staggered conformation in **1** are not intrinsic features of *trans*-$Fe(CO)_3(PR_3)_2$ complexes but are consequences of the phosphine substitution pattern and its effects on crystal packing.

Acknowledgment is made to the donors of the Petroleum Research Fund, administered by the American Chemical Society, and the MU Research Council for support of this research. The theoretical work was carried out at the NSF Supercomputer Center at the University of Illinois and at the MU Campus Computer Center. The X-ray diffractometer was partially funded by the National Science Foundation (CHE 90–11804). G.S.C. gratefully acknowledges support by a Bent Fellowship. We thank Drs. Richard and Ellen Keiter for helpful comments, suggestions, and discussions and Steve Meyer for software installations on the IBM cluster.

Supplementary Material Available: Complete set of tables of crystal data, bond distances and angles, positional and thermal parameters, anisotropic thermal parameters, H-atom parameters, and orthogonalization matrix and coordinates and ORTEP drawings for **1** (18 pages). Ordering information is given on any current masthead page. This material including structure factors can be obtained on request from the Director, Cambridge Crystallographic Data Centre, 12 Union Road, Cambridge, CB2 1EZ, UK.

OM930873K